Supplemental Material

© Copyright 2020 American Meteorological Society
Permission to use figures, tables, and brief excerpts from this work in scientific and educational works is hereby granted provided that the source is acknowledged. Any use of material in this work that is determined to be “fair use” under Section 107 of the U.S. Copyright Act or that satisfies the conditions specified in Section 108 of the U.S. Copyright Act (17 USC §108) does not require the AMS’s permission. Republication, systematic reproduction, posting in electronic form, such as on a website or in a searchable database, or other uses of this material, except as exempted by the above statement, requires written permission or a license from the AMS. All AMS journals and monograph publications are registered with the Copyright Clearance Center (http://www.copyright.com). Questions about permission to use materials for which AMS holds the copyright can also be directed to permissions@ametsoc.org. Additional details are provided in the AMS Copyright Policy statement, available on the AMS website (http://www.ametsoc.org/CopyrightInformation).

Supplementary Information for

Atmospheric radiative processes accelerate ground surface warming over the southeastern Tibetan Plateau during 1998-2013

Peng Ji[1,2], Xing Yuan[1,3,*] and Dan Li[4]

[1]Key Laboratory of Regional Climate-Environment for Temperate East Asia, Institute of Atmospheric Physics, Chinese Academy of Sciences, Beijing 100029, China

[2]College of Earth and Planetary Sciences, University of Chinese Academy of Sciences, Beijing 100049, China

[3]School of Hydrology and Water Resources, Nanjing University of Information Science and Technology, Nanjing 210044, China

[4]Department of Earth and Environment, Boston University, Boston, MA 02215, USA

Submitted to *Journal of Climate*

June 2, 2019

Revised September 17, 2019

Revised November 17, 2019

*Corresponding author address: Xing Yuan, School of Hydrology and Water Resources, Nanjing University of Information Science and Technology, Nanjing 210044, Jiangsu, China. E-mail: xyuan@nuist.edu.cn

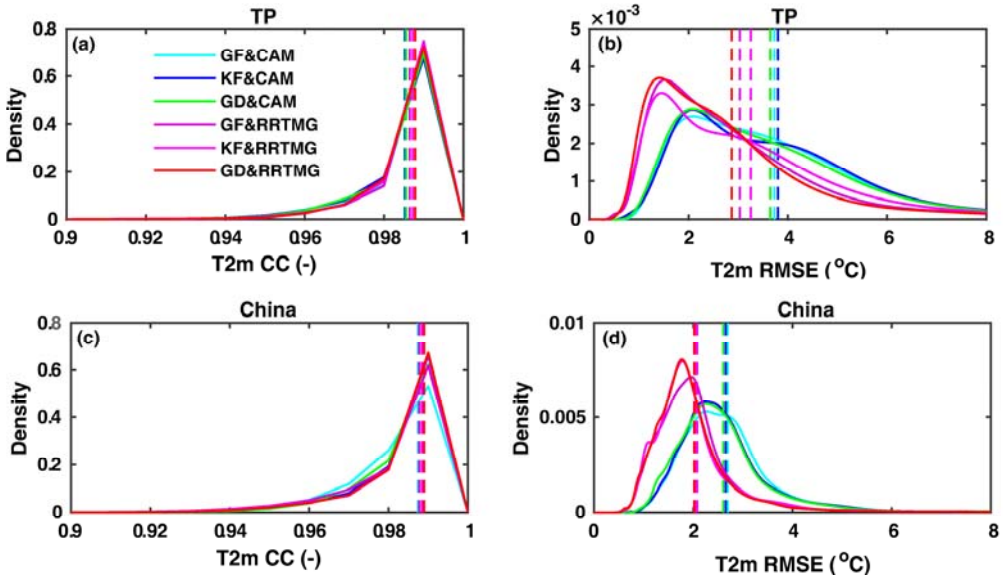

Fig. S1. Evaluation of six physical configurations of WRF model including three cumulus parameterizations (GF: Grell-Freitas scheme, GD: Grell-Devenyi ensemble scheme, and KF: Kain-Fritsch scheme) and two radiation transfer schemes (CAM and RRTMG). (a) Solid lines show probability distribution functions of correlation coefficient (CC) between simulated and observed monthly temperature over the Tibetan Plateau, while dashed lines are mean values. (b) The same as (a), but for the root mean squared error (RMSE). (c-d) are the same as (a-b) but for the whole China. CC and RMSE are calculated over each station during 1998 and 2006, and the probability distribution functions of CC and RMSE are estimated by using the Kernel density estimation.

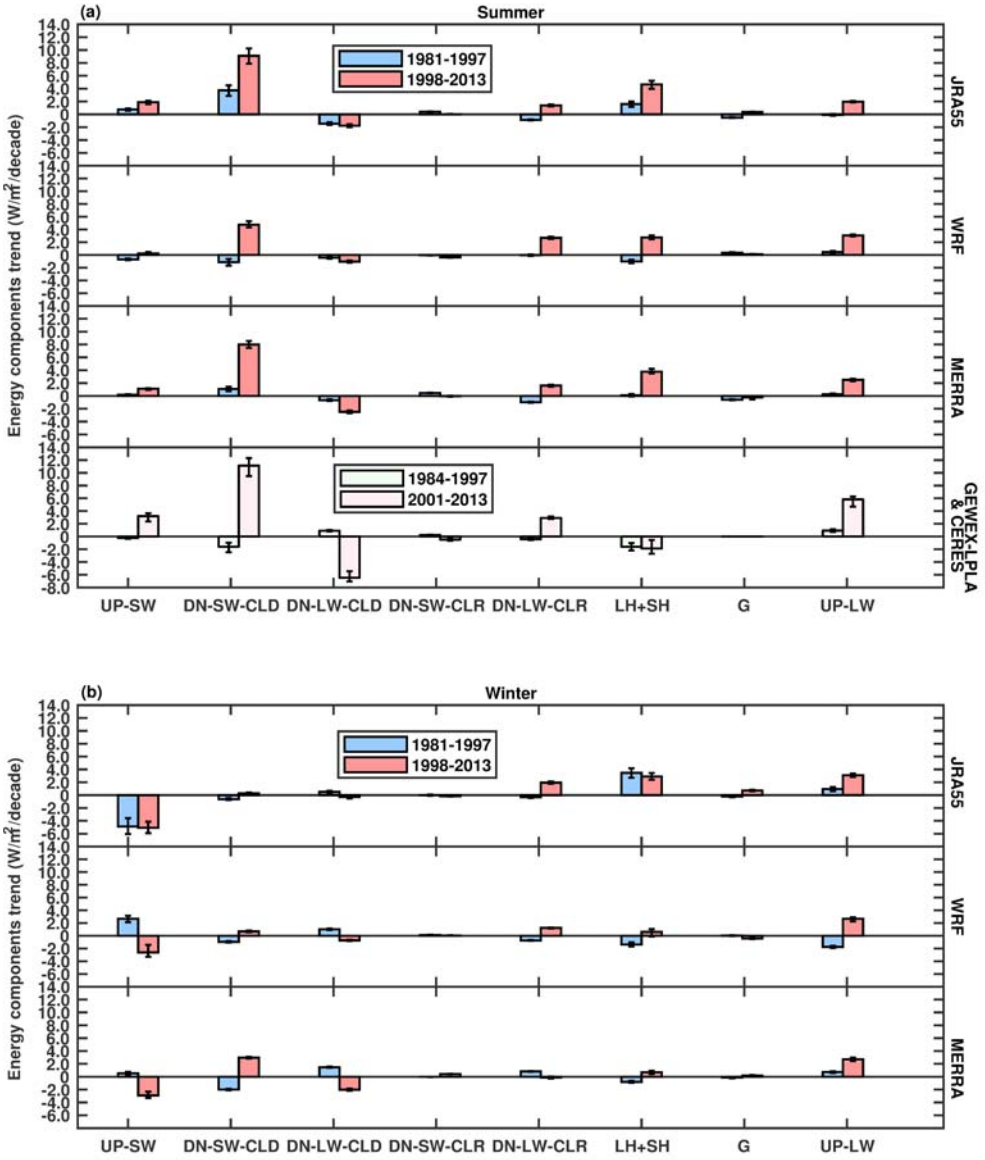

Fig. S2. Linear trends of different surface energy balance components during the (a) summer and (b) winter of 1981-1997 and 1998-2013. Surface energy balance components include surface upward shortwave radiation (UP-SW), surface downward cloudy-sky (DN-SW-CLD) and clear-sky (DN-SW-CLR) shortwave radiations, surface downward cloudy-sky (DN-LW-CLD) and clear-sky (DN-LW-CLR) longwave radiations, latent and sensible heat fluxes (LH+SH), ground heat flux (G)

and surface upward longwave radiation (UP-LW). Black bars represent uncertainties at 95% confidence level.

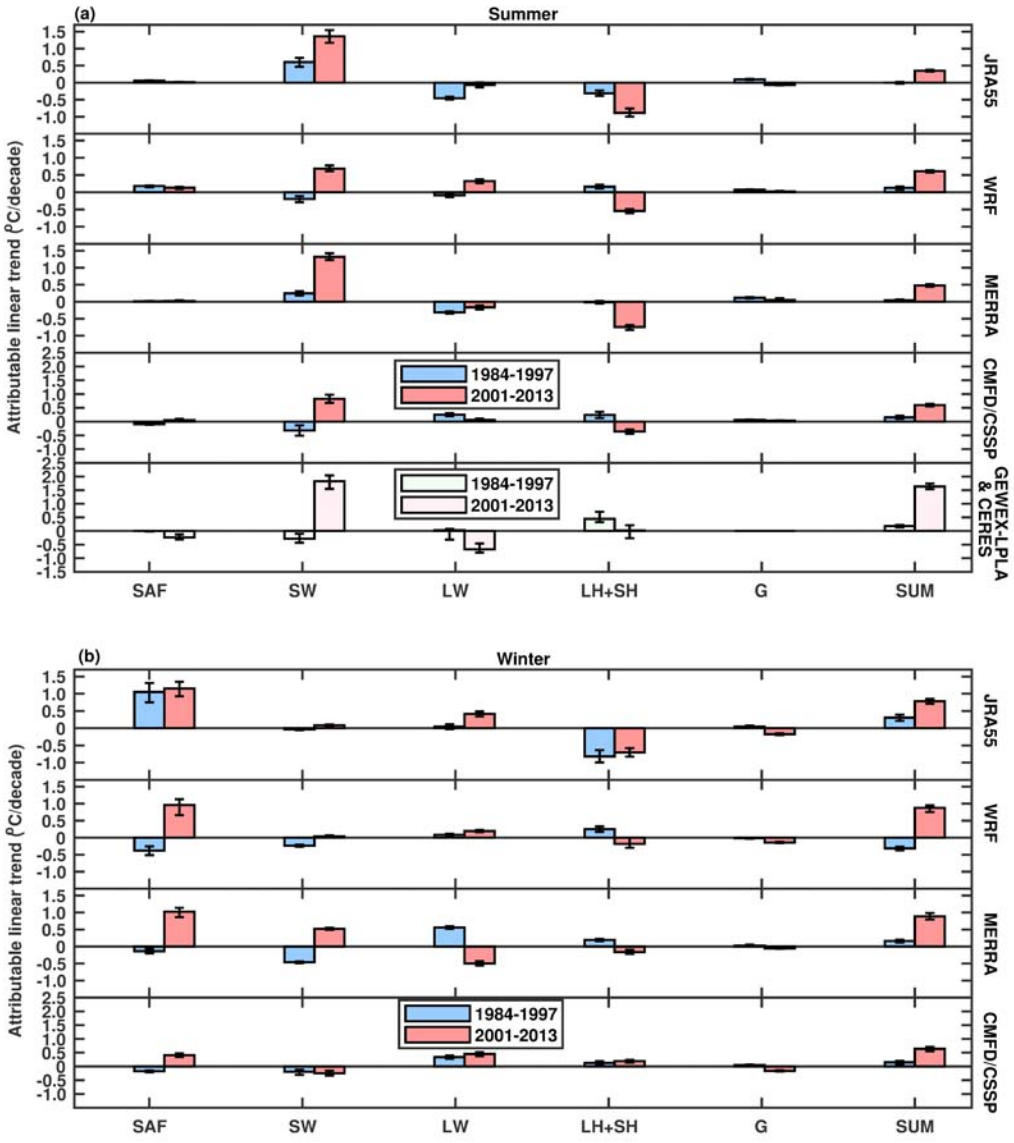

Fig. S3. Contributions from surface albedo (SAF), shortwave radiation (SW), longwave radiation (LW), latent and sensible heat flux (LH+SH) and ground heat flux (G) during the (a) summer and (b) winter of 1981-1997 and 1998-2013. The SUM means integrated trends from all radiative factors. Black bars represent sampling uncertainties at 95% confidence level.

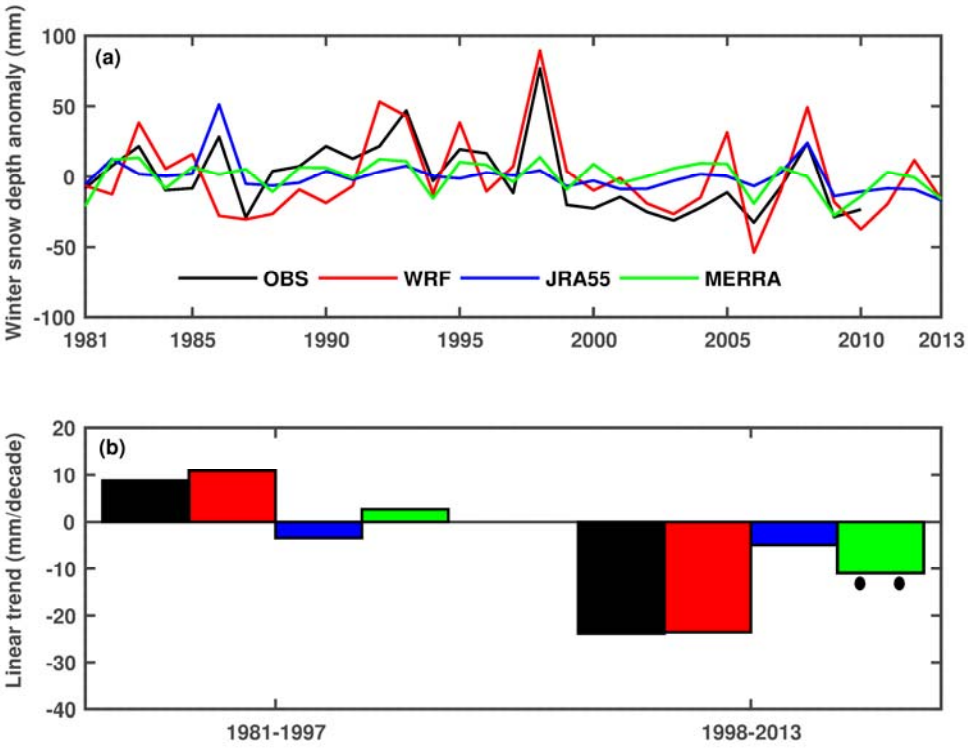

Fig. S4. (a) Observed and simulated snow depth anomalies during winter season averaged over the southeastern TP.. (b) Linear trends of snow depth during 1981-1997 and 1998-2013. Two dots are significance at the 95% confidence levels.

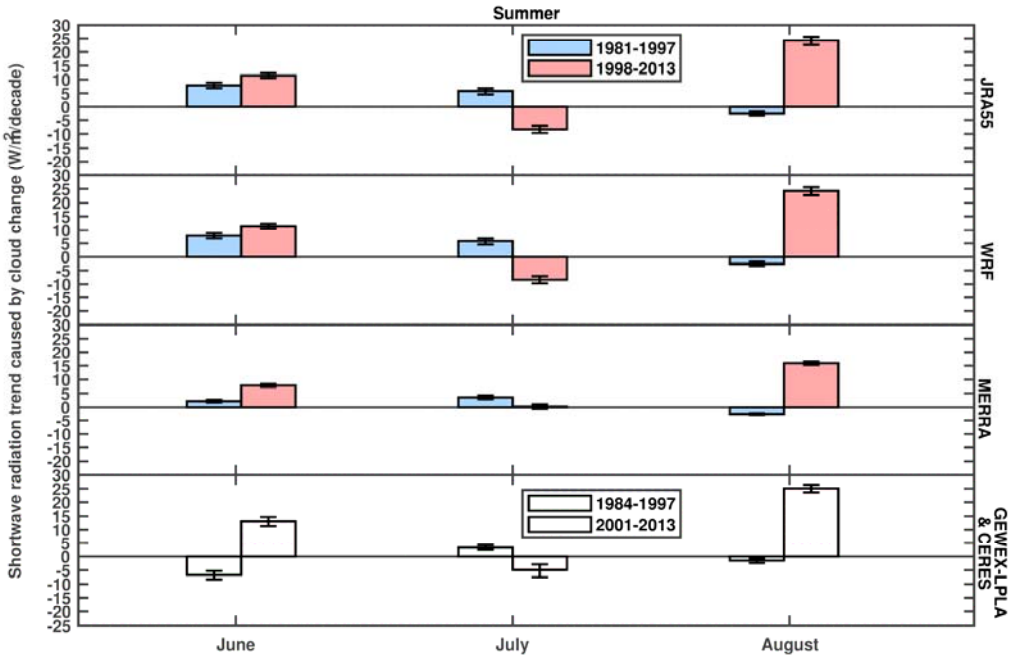

Fig. S5. Linear trends of surface downward cloudy-sky shortwave radiation during 1981-1997 and 1998-2013 in June, July and August.

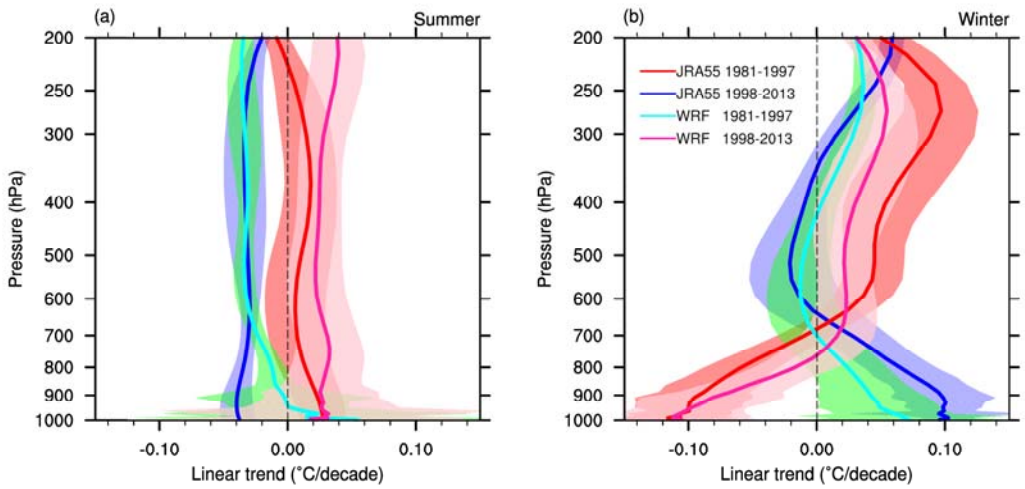

Fig. S6. The same as Fig. 11 but for southeastern China.

.

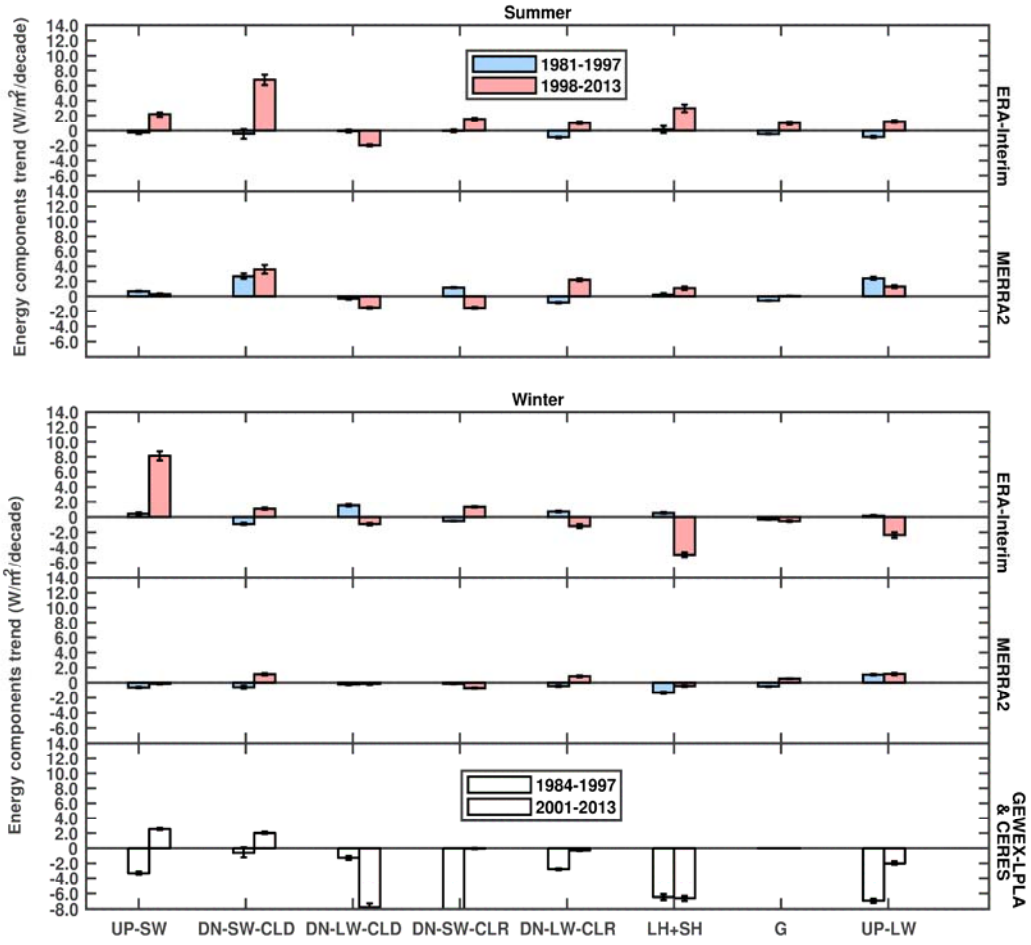

Fig. S7. The same as Fig. S2, but for the ERA-Interim, MERRA2, GEWEX-LPLA and CERES datasets.